Localized surface plasmon enhanced cathodoluminescence from Eu^{3+}-doped phosphor near the nanoscaled silver particles

Seong Min Lee,[1] Kyung Cheol Choi,[1,*] Dong Hyuk Kim,[2] and Duk Young Jeon[2]

[1]*Department of Electrical Engineering, KAIST, Yuseong-gu, Daejeon 305-701, Korea*
[2]*Department of Materials Science and Engineering, KAIST, Yuseong-gu, Daejeon 305-701, Korea*
**kyungcc@kaist.ac.kr*

Abstract: We elucidate that the luminescence from Eu^{3+}-doped phosphor excited by the electron collision can be modified on location near the metallic nanoparticles. The Eu^{3+}-doped phosphor was fabricated on the nanoscaled Ag particles ranging of 5 nm to 30 nm diameter. As a result of the cathodoluminescence measurements, the phosphor films on the Ag particles showed up to twofold more than that of an isolated phosphor film. Enhanced cathodoluminescence originated from the resonant coupling between the localized surface plasmon of Ag nanoparticles and radiating energy of the phosphor. Cathodoluminescent phosphor for high luminous display devices can be addressed by locating phosphor near the surface of metallic nanoparticles.

OCIS codes: (250.5403) Plasmonics; (250.1500) Cathodoluminescence.

References and links

1. S. M. Lee and K. C. Choi, "Enhanced emission from $BaMgAl_{10}O_{17}:Eu^{2+}$ by localized surface plasmon resonance of silver particles," Opt. Express **18**(12), 12144–12152 (2010).
2. J. R. Lakowicz, "Plasmonics in biology and plasmon-controlled fluorescence," Plasmonics **1**(1), 5–33 (2006).
3. E. Ozbay, "Plasmonics: merging photonics and electronics at nanoscale dimensions," Science **311**(5758), 189–193 (2006).
4. B. Moine and G. Bizarri, "Rare-earth doped phosphors: oldies or goldies?" Mater. Sci. Eng. B **105**(1-3), 2–7 (2003).
5. T. Hayakawa, K. Furuhashi, and M. Nogami, "Enhancement of $^5D_0$-^7F_J emissions of Eu^{3+} ions in the vicinity of polymer-protected Au nanoparticles in sol–gel-derived B_2O_3–SiO_2 glass," J. Phys. Chem. B **108**(31), 11301–11307 (2004).
6. R. Reisfeld, M. Pietraszkiewicz, T. Saraidarov, and V. Levchenko, "Luminescence intensification of lanthanide complexes by silver nanoparticles incorporated in sol-gel matrix," J. Rare Earths **27**(4), 544–549 (2009).
7. J. Zhu, "Enhanced fluorescence from Dy^{3+} owing to surface plasmon resonance of Au colloid nanoparticles," Mater. Lett. **59**(11), 1413–1416 (2005).
8. X. Fang, H. Song, L. Xie, Q. Liu, H. Zhang, X. Bai, B. Dong, Y. Wang, and W. Han, "Origin of luminescence enhancement and quenching of europium complex in solution phase containing Ag nanoparticles," J. Chem. Phys. **131**(5), 054506 (2009).
9. Y. Wang, J. Zhou, and T. Wang, "Enhanced luminescence from europium complex owing to surface plasmon resonance of silver nanoparticles," Mater. Lett. **62**(12-13), 1937–1940 (2008).
10. K. Y. Yang, K. C. Choi, and C. W. Ahn, "Surface plasmon-enhanced spontaneous emission rate in an organic light-emitting device structure: cathode structure for plasmonic application," Appl. Phys. Lett. **94**(17), 173301 (2009).
11. K. Y. Yang, K. C. Choi, and C. W. Ahn, "Surface plasmon-enhanced energy transfer in an organic light-emitting device structure," Opt. Express **17**(14), 11495–11504 (2009).
12. W. A. Murray and W. L. Barnes, "Plasmonic materials," Adv. Mater. (Deerfield Beach Fla.) **19**(22), 3771–3782 (2007).
13. K. H. Cho, S. I. Ahn, S. M. Lee, C. S. Choi, and K. C. Choi, "Surface plasmonic controllable enhanced emission from the intrachain and interchain excitons of a conjugated polymer," Appl. Phys. Lett. **97**(19), 193306 (2010).
14. J. H. Kang, M. Nazarov, W. B. Im, J. Y. Kim, and D. Y. Jeon, "Characterization of nano-size YVO_4:Eu and (Y,Gd)VO_4:Eu phosphors by low voltage cathodo- and photoluminescence," J. Vac. Sci. Technol. B **23**(2), 843–848 (2005).
15. C. C. Wu, K. B. Chen, C. S. Lee, T. M. Chen, and B. M. Cheng, "Synthesis and VUV photoluminescence characterization of (Y, Gd)(V, P)O_4:Eu^{3+} as a potential red-emitting PDP phosphor," Chem. Mater. **19**(13), 3278–3285 (2007).

#145138 - $15.00 USD Received 19 Apr 2011; revised 13 Jun 2011; accepted 14 Jun 2011; published 23 Jun 2011

16. A. K. Levine and F. C. Palilla, "A new, highly efficient red-emitting cathodoluminescent phosphor (YVO_4:Eu) for color television," Appl. Phys. Lett. **5**(6), 118–120 (1964).
17. T. Hayakawa, S. T. Selvan, and M. Nogami, "Field enhancement effect of small Ag particles on the fluorescence from Eu^{3+}-doped SiO_2 glass," Appl. Phys. Lett. **74**(11), 1513–1515 (1999).
18. V. Bulović, V. Khalfin, G. Gu, P. Burrows, D. Garbuzov, and S. Forrest, "Weak microcavity effects in organic light-emitting devices," Phys. Rev. B **58**(7), 3730–3740 (1998).
19. K. Matsubara, H. Tampo, H. Shibata, A. Yamada, P. Fons, K. Iwata, and S. Niki, "Band-gap modified Al-doped $Zn_{1-x}Mg_xO$ transparent conducting films deposited by pulsed laser deposition," Appl. Phys. Lett. **85**(8), 1374–1376 (2004).
20. T. Hayakawa, S. Tamil Selvan, and M. Nogami, "Enhanced fluorescence from Eu^{3+} owing to surface plasma oscillation of silver particles in glass," J. Non-Cryst. Solids **259**(1-3), 16–22 (1999).
21. M. S. Elmanharawy, A. H. Eid, and A. A. Kader, "Spectra of europium-doped yttrium oxide and yttrium vanadate phosphors," Czech. J. Phys. **28**(10), 1164–1173 (1978).
22. N. Noginova, Y. Barnakov, H. Li, and M. A. Noginov, "Effect of metallic surface on electric dipole and magnetic dipole emission transitions in Eu^{3+} doped polymeric film," Opt. Express **17**(13), 10767–10772 (2009).
23. B. J. Lawrie, R. F. Haglund, Jr., and R. Mu, "Enhancement of ZnO photoluminescence by localized and propagating surface plasmons," Opt. Express **17**(4), 2565–2572 (2009).
24. K. Okamoto, I. Niki, A. Shvartser, Y. Narukawa, T. Mukai, and A. Scherer, "Surface plasmon enhanced super bright InGaN light emitter," Phys. Status Solidi C **2**(7), 2841–2844 (2005).
25. K. Okamoto, I. Niki, A. Shvartser, Y. Narukawa, T. Mukai, and A. Scherer, "Surface-plasmon-enhanced light emitters based on InGaN quantum wells," Nat. Mater. **3**(9), 601–605 (2004).

1. Introduction

Localized surface plasmon resonance has attracted immense interest from many material science researchers of rare-earth ions such as europium (Eu), terbium (Tb), and dysprosium (Dy) [1]. Although rare-earth ions construct a luminescent center in biological sensing, fluorescence imaging analysis, and display phosphors, the efficacy of their luminescence has not yet been addressed [2–5]. The localized surface plasmon induced by a metallic nanostructure can enhance the intensity of the photoluminescence of rare-earth ions [1]. Some studies have examined the enhanced photoluminescence of rare-earth ions by using the localized surface plasmon induced by metallic particles [6–9]. Reisfeld et al. showed that the luminescence of Eu complexes can be increased when the electronic levels of the Eu complex interact with the radiation field of silver (Ag) nanoparticles [6]. Zhu showed that the enhanced fluorescence of Dy^{3+} ions is due to the localized surface plasmon of Au colloidal nanoparticles [7]. In addition, Fang et al. [8] and Wang et al. [9] reported that the luminescence of Eu^{3+} ions dispersed in a solution could be enhanced when Ag nanoparticles are mixed in the solution. However, most of the existing works are limited to the emission intensity of pure rare-earth ions in the solution phase. Moreover, studies on enhanced luminescence mainly involve the use of rare-earth ions under optical excitation of ultraviolet light. The results of those studies fail to show the challenges of utilizing rare-earth ions in commercial display devices [9–11].

We demonstrate how metal-induced plasmon can enhance the cathodoluminescence of a rare-earth ion doped phosphor system that is used in commercial display devices, such as a field emission display or a carbon nanotube backlight unit. We used Ag nanoparticles as the plasmon inducer and introduced a dielectric spacer to prevent luminescence quenching. Up to twofold enhancement factor was obtained when the Ag nanoparticles were evaporated to a thickness of 3.5 nm and spaced 20 nm from the light emitter. In addition, the distance dependency on the plasmon-enhanced luminescence was investigated by varying the spacer thickness in a range of 0 nm to 80 nm. The fact that the emission level is intensified as a result of the excitation caused by a collision with an electron beam is an important finding since the first report in self-emissive display technology.

2. Experimental

We used the test sample for the cathodoluminescence (CL) measurement as shown in Fig. 1. The multilayer test sample consists of a phosphor layer (top), a dielectric spacer, Ag nanoparticles, and a glass substrate coated with indium tin oxide (ITO, bottom). The ITO-coated glass was selected for the adhesion of Ag particles and the front structure of field emission displays. To induce localized surface plasmon resonance near the phosphor, we fabricated the Ag nanoparticles (up to several dozen nanometers in size) below the phosphor

#145138 - $15.00 USD Received 19 Apr 2011; revised 13 Jun 2011; accepted 14 Jun 2011; published 23 Jun 2011

layer by thermal evaporation method. The Ag nanoparticles were evaporated to a deposition thickness ranging from 0 nm to 3.5 nm at a constant rate of 0.1 Å/s. The Ag nanoparticles were fabricated randomly as a way of ignoring the resonant interaction between the metallic particles. As a dielectric spacer, magnesium oxide (MgO) was inserted between the phosphor layer and the Ag particles. In this work, the dielectric spacer physically separates the light matter and the Ag particles. We deposited the MgO spacer by means of e-beam evaporation. The MgO spacer was evaporated to a deposition thickness ranging from 0 nm to 80 nm at a constant rate of 0.3 Å/s. The phosphor material used in this work is $YVO_4:Eu^{3+}$; it was manufactured in the form of a transparent thin film. A 100 nm thick layer of $YVO_4:Eu^{3+}$ was deposited on the spacer, Ag particles, and ITO-coated glass by means of a RF magnetron sputter at 150°C. The thickness measurements presented in this paper were obtained by using a quartz crystal oscillator as a deposition monitor. The surface morphology of the evaporated Ag nanoparticles was determined via scanning electron microscopy (SEM) with a FEI (Netherlands) Sirion microscope. In addition, the influence of Ag nanoparticle on the surface roughness of thin film phosphor was determined with the aid of Atomic Force Microscope with a NanoMan AFM (Veeco, USA). The CL measurements were taken by a SEM with a Gatan MonoCL3 system. The phosphor samples were excited by an electron beam from an electron gun under an acceleration voltage of 5 kV and an electron beam current of 10.1 μA. The localized surface plasmon resonance can be resulted in extinct of incident electromagnetic wave. Thus, the extinction spectra enabled us to study the plasmonic resonance caused by metallic nanoparticles [12]. An extinction spectrum of the Ag particles was obtained with a Shimadzu spectrophotometer (UV-2550, Japan).

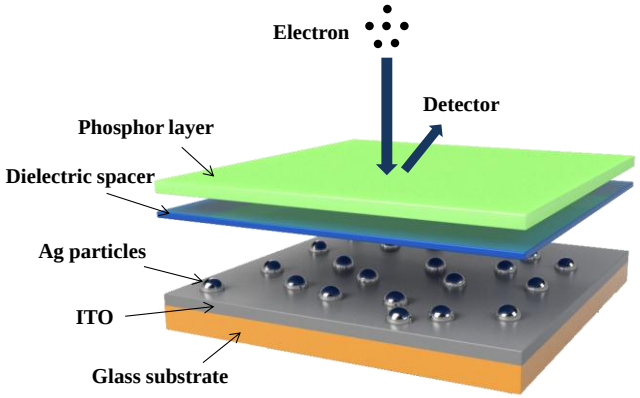

Fig. 1. Graphical representation of the multilayer test sample: the phosphor layer, the dielectric spacer (MgO), the Ag nanoparticles, and the ITO-coated glass substrate.

The surface status of randomly fabricated Ag nanoparticles in the present work was confirmed through the SEM images shown in Fig. 2. The Ag particles were randomly deposited on the substrate to a thickness of 0.5 nm to 3.5 nm after thermal evaporation at a constant deposition rate. At a deposition thickness of 0.5 nm, the fabricated Ag particles had a near-spherical shape with an average of 5 nm diameter. When the deposition thickness reached 3.5 nm, the diameter of the Ag particles expanded to an average of 30 nm. The distribution of the Ag particles also became dense, and the voids between the particles disappeared. At this range of deposition thickness, the Ag particles failed to form a continuous film; instead, they formed a cluster of isolated islands [13].

#145138 - $15.00 USD Received 19 Apr 2011; revised 13 Jun 2011; accepted 14 Jun 2011; published 23 Jun 2011

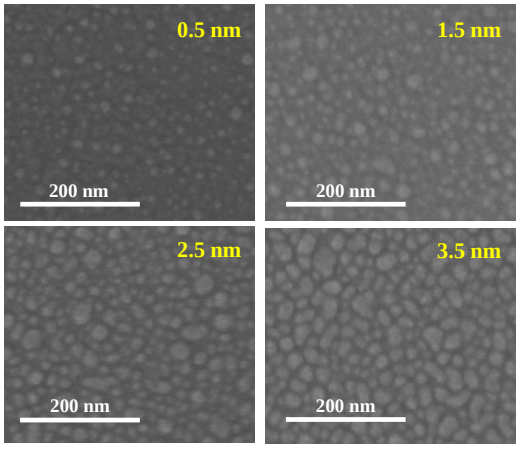

Fig. 2. SEM images of Ag particles thermally evaporated on an ITO-coated glass substrate for the following deposition thicknesses: (a) 0.5 nm, (b) 1.5 nm, (c) 2.5 nm, and (d) 3.5 nm, at constant rate of 0.1 Å/s.

Figure 3 shows the extinction spectra of randomly fabricated Ag nanoparticles in relation to the evaporation thickness. The extinction spectra were measured under the fully fabricated sample structure: the Ag particles were surrounded by a dielectric spacer (MgO) and ITO-coated glass. The localized surface plasmon resonance can be modified according to the dielectric materials around the metal particles. The extinction peak of the Ag nanoparticles inserted between the MgO and ITO layers moved from 470 nm to 560 nm as the deposition thickness of the Ag nanoparticles increased. The extinction spectrum of the Ag particles was red-shifted and the half-bandwidth became broad; this behavior is remarkably in line with the increase in size and distribution of the Ag particles. Moreover, the extinction spectra that show an increase in the thickness of the Ag particle deposition deeply overlap the emission area of the Eu^{3+}-doped phosphor.

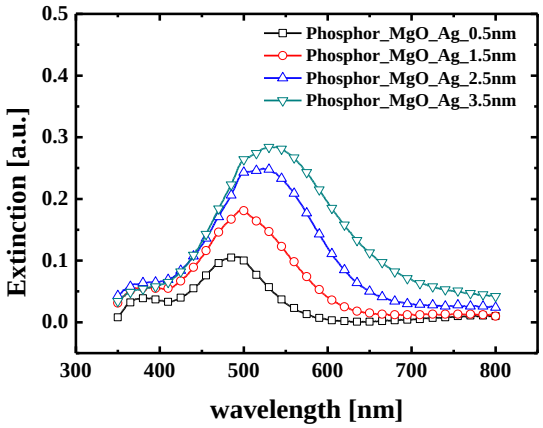

Fig. 3. The extinction spectra of Ag particles surrounded by a dielectric spacer (MgO) and the ITO-coated glass substrate for the following deposition thicknesses: (a) 0.5 nm, (b) 1.5 nm, (c) 2.5 nm, and (d) 3.5 nm.

3. Results and discussion: CL spectra of Eu^{3+}-doped phosphor

Figure 4 depicts the CL spectra of phosphor films measured under the excitation of a collision with an energetic electron beam and wavelength-dependent enhancement factors. Among a few of radiation peaks of the Eu^{3+} ions, we focused on two radiation peaks: a magnetic dipole

#145138 - $15.00 USD Received 19 Apr 2011; revised 13 Jun 2011; accepted 14 Jun 2011; published 23 Jun 2011

transition at 590 nm and an electric dipole transition at 620 nm [14]. The Eu^{3+} ion is radiated by the transition process of 4f-4f orbital electrons [15,16]. Since 4f electrons are electrically shielded by electrons on the 5s and 5p orbit, the luminescent spectrum of Eu^{3+} ions is not dominantly governed by the host matrix. The CL intensity in Fig. 4(a) was plotted in relation to the thickness of the Ag particle deposition at a distance of 20 nm from the dielectric spacer; the reference for the plotting was isolated from the Ag particles. The emission intensity of phosphor deposited on the Ag particles increased as the thickness of the Ag particle deposition increased. The increased part of the emission wavelength was mainly observed at around 620 nm. Furthermore, although the emission intensity showed a significant difference on the existence of Ag particles, the spectral position of the radiation peaks remained constant. This behavior implies that the emission wavelength of phosphor was not modified by the insertion of Ag particles. Figure 4(b) shows that the enhancement at 620 nm by electric dipole transition is higher than that at 590 nm by magnetic dipole transition. At 3.5 nm of Ag evaporation, the difference in wavelength-dependent enhancement gets larger. To explore the possibility that this enhancement originates from the localized surface plasmon resonance of Ag nanoparticles, we calculated the asymmetric ratio by dividing the integrated intensity around 620 nm by the integrated intensity around 590 nm. The asymmetric ratio of Eu^{3+} ions that is reflected by the increase or decrease in luminescence can be changed by coupling it with the plasmon resonance [17]. Therefore, this can be used as good evidence for detecting the localized plasmon medicated luminescence. As shown in the inset figure of Fig. 4(b), the asymmetric ratio of up to 1.5 nm of Ag nanoparticles is the same as the reference, while the asymmetric ratio increased after 2.5 nm of Ag nanoparticles that the CL intensity increased significantly. Therefore, the enhanced cathodoluminescence is due to the increased asymmetric ratio from the Ag nanoparticles.

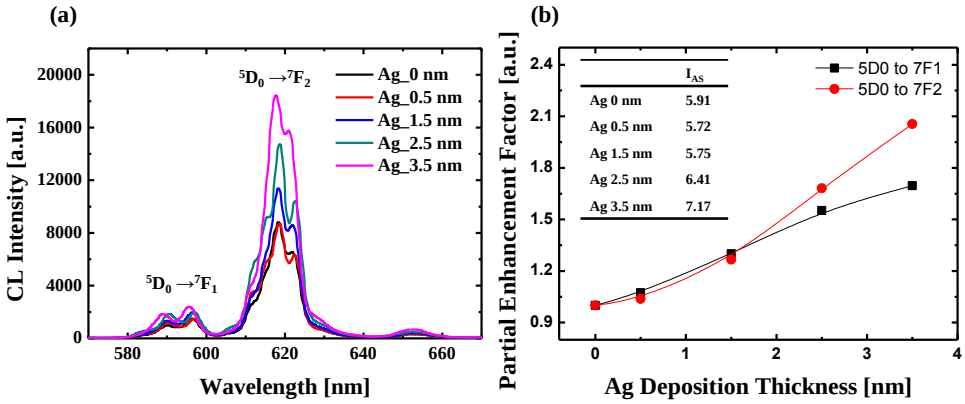

Fig. 4. (a) CL spectra taken at a dielectric spacer distance of 20 nm between the phosphor layer and the Ag nanoparticles for the following deposition thicknesses: 0 nm, 0.5 nm, 1.5 nm, 2.5 nm, and 3.5 nm, (b) partially integrated enhancement factors at magnetic and electric dipole transitions. (The inset figure shows asymmetric ratios, which are calculated by $I_{AS} = \frac{\int_{0\rightarrow 2} I(\omega)d\omega}{\int_{0\rightarrow 1} I(\omega)d\omega}$.)

Figure 5 shows the enhancement factor of the emission intensity of Eu^{3+}-doped phosphor films as a function of the thicknesses of the Ag nanoparticle deposition and the MgO dielectric spacer. The enhancement factor was obtained by dividing the integrated emission intensity of a sample with Ag nanoparticles by the integrated emission intensity of a reference sample without Ag nanoparticles and a dielectric spacer. Figure 5(a) shows how the thickness of the Ag nanoparticle deposition affects the enhancement factor of the emission intensity when the thickness of the dielectric spacer is restricted to 20 nm. The enhancement factor increases as the thickness of the Ag nanoparticle deposition increases. At a deposition thickness of 3.5 nm, the enhancement factor increased up to 1.92 times. Figure 5(b) shows

#145138 - $15.00 USD Received 19 Apr 2011; revised 13 Jun 2011; accepted 14 Jun 2011; published 23 Jun 2011

how the dielectric spacer influences the emission enhancement when the thickness of the Ag nanoparticle deposition is 3.5 nm. In other words, the enhancement factor in Fig. 5(b) depends on the distance between the light emitter and the Ag nanoparticles. Initially the enhancement factor of the sample without Ag nanoparticles (square) is constant, regardless of the MgO thickness. The thickness of the dielectric spacer does not change the emission intensity of the Eu^{3+}-doped phosphor. In contrast, the enhancement factor of the sample with Ag nanoparticles (circle) reaches its maximum level at an MgO thickness of 20 nm; after that, the enhancement factor decreases as the MgO thickness increases. The enhancement effect by the localized surface plasmon became weaker for MgO thicknesses of up to 80 nm. Note that there was no increase in the emission of the sample with Ag nanoparticles when the particles and light emitter were not separated by the dielectric spacer. That is the reason the luminescence can be quenched in the case of direct contact between the Ag nanoparticles and the light emitter.

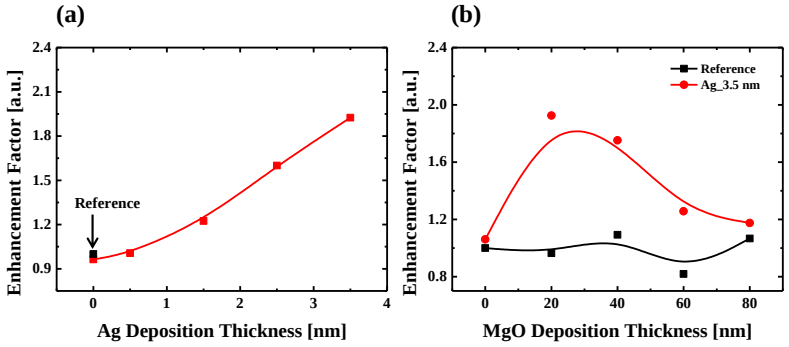

Fig. 5. The enhancement factors of the integrated CL intensity in relation to (a) the thickness of the evaporated Ag and (b) the thickness of the dielectric spacer; and comparison of this ratio with that of the reference sample without Ag nanoparticles.

The enhancement factor calculated in Fig. 5 can potentially change; owing to the Ag nanoparticles, the potential change is more likely to be caused by the surface morphology than the localized surface plasmon. To observe the surface morphology of the sample structure, we used an atomic force microscope (AFM) to measure the roughness of a three-dimensional cross section. The roughness of a 1 μm^2 area is calculated by the root mean square. Figure 6 shows that the phosphor films used in this work have a rough surface. Because of the difficulty of distinguishing surface morphologies in three-dimensional AFM images, we present the root mean square values of the roughness in Table 1. The reference sample without the Ag nanoparticles or the dielectric spacer had a roughness of about 4.6 nm due to the phosphor deposition. When the thickness of the MgO and Ag nanoparticle deposition is increased, the differences of roughness are just 3.15 nm and 1.15 nm, respectively. The difference in surface roughness can be negligible in relation to the total thickness of the prepared sample.

#145138 - $15.00 USD Received 19 Apr 2011; revised 13 Jun 2011; accepted 14 Jun 2011; published 23 Jun 2011

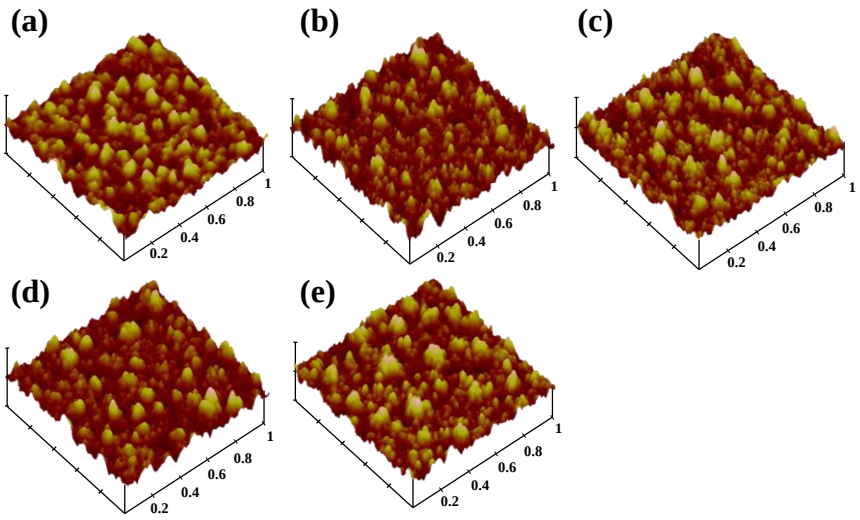

Fig. 6. The three-dimensional AFM images of the surface roughness of the fully fabricated samples for the following thicknesses of Ag nanoparticles deposition: (a) 0 nm, (b) 0.5 nm, (c) 1.5 nm, (d) 2.5 nm, and (e) 3.5 nm, all samples have an MgO spacer of 20 nm. The measured area is 1 μm^2.

Table 1. The Calculated Surface Roughness from AFM Measurements of the Phosphor Film as the Following Thicknesses of Ag Nanoparticles and an MgO Deposition*

	MgO_0 nm	MgO_20 nm	MgO_40 nm	MgO_60 nm	MgO_80 nm
Ag_0 nm	4.624	4.831	7.772	5.925	6.629

	Ag_0 nm	Ag_0.5 nm	Ag_1.5 nm	Ag_2.5 nm	Ag_3.5 nm
MgO_20 nm	4.831	5.731	4.928	5.984	5.720

Unit: nm

*The roughness values are derived from the root mean square.

To understand the local field enhancement of electromagnetic near-fields due to Ag nanoparticles, we carried out Finite Deference Time Domain (FDTD) calculation. Figure 7(a) shows a schematic diagram for numerical analysis that uses the FDTD [1]. For an approximate, Eu^{3+} ion doped phosphor was modeled as a 620 nm emitting point dipole. Also, an Ag nanoparticle with a diameter of 30 nm based on SEM images shown in Fig. 2, which is assumed to have a spherical shape, was placed 2 nm from the point dipole. The Ag nanoparticle was located on the border between MgO and ITO layers. The point dipole source was perpendicularly oriented to the metal surface along the Z axis. Figure 7(b) shows the electric field distribution of only the isolated dipole source without any Ag nanoparticles, while Fig. 7(c) shows the electric field distribution in the presence of an Ag nanoparticle. Finally, Fig. 7(d) shows the ratios of the enhanced or quenched electric field intensity in the X-Z plane around the Ag nanoparticle. Here, the local field enhancement factors were estimated by dividing the field intensity in the presence of an Ag nanoparticle by the field intensity of an isolated phosphor. All of the figures were represented in a logarithmic scale (base 10) for clarity. As shown in Fig. 7(d), the near-field distribution of the emitting dipole in the presence of Ag nanoparticles increased drastically. It is noteworthy that the enhancement occurred when the Ag nanoparticle was embedded in MgO and ITO. This result means that the Ag nanoparticle surrounded by a higher refractive index of MgO (n = 1.74) and ITO (n = 1.8) than air (n = 1) had a resonance with a red emission centered at 620 nm [18,19].

#145138 - $15.00 USD Received 19 Apr 2011; revised 13 Jun 2011; accepted 14 Jun 2011; published 23 Jun 2011

Therefore, we believe that the Ag nanoparticle used in the present experiment can have a plasmon resonance with a Eu^{3+}-doped phosphor, compared with the theoretical calculation.

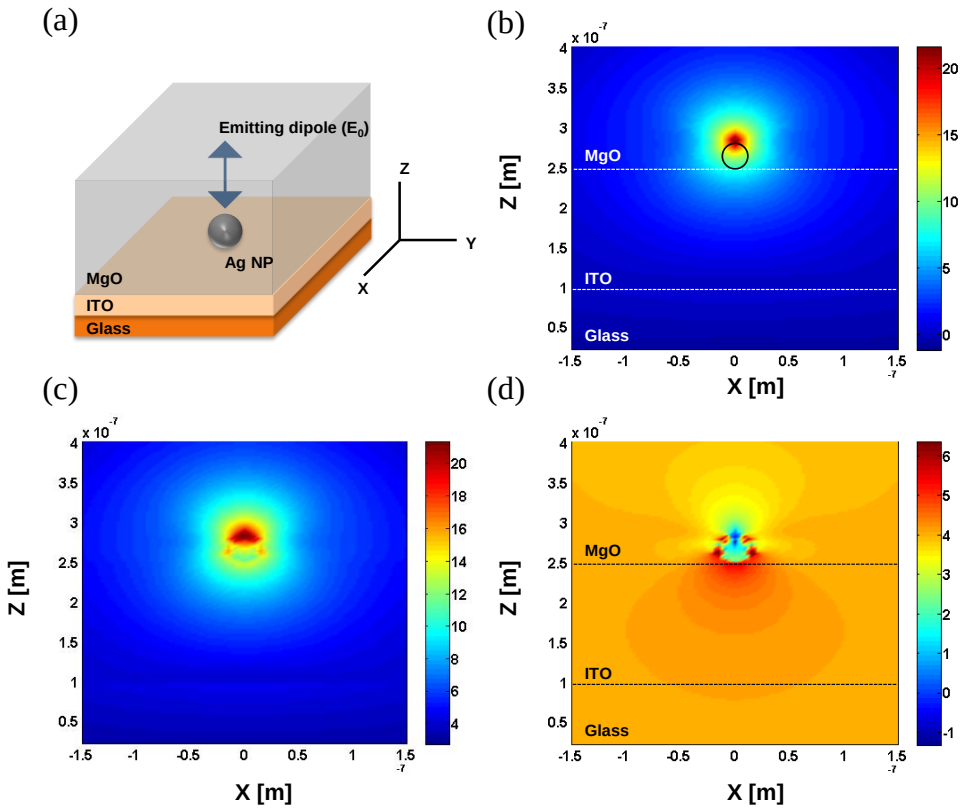

Fig. 7. Numerical analysis of the localized field enhancement on the resonance of an Ag nanoparticle and the emitting dipole under the sample structure, (a) simulation configuration for the FDTD calculation and the near-field distribution around this, (b) an isolated 620 nm-radiating dipole, (c) the diameter of 30 nm of an Ag nanoparticle placed 2 nm from the radiating dipole, and (d) the enhanced/quenched electric field intensity.

In this work, we revealed that Ag nanoparticles can modify the CL of Eu^{3+}-doped phosphor in close proximity to the surface of the Ag nanoparticles. When the phosphor is deposited on Ag nanoparticles surrounded by a 20 nm of MgO dielectric spacer, the emission intensity of the sample with a 3.5 nm of Ag nanoparticles is 1.92 times larger than that of the reference sample. We believe that this enhancement originates from the localized surface plasmon resonance caused by the Ag nanoparticles. The extinction spectra show that the plasmon resonance peak of the Ag nanoparticles is moved toward a long wavelength. This behavior is due to an increase in the size of the Ag nanoparticles and a decrease in the voids among the Ag nanoparticles. At an Ag nanoparticle deposition thickness of 3.5 nm, the plasmon band of Ag nanoparticles deeply overlaps with the red emission of the Eu^{3+}-doped phosphor, which means there is strong resonant coupling between the Ag nanoparticles and the excited species under irradiation from the energetic electron beam. When Eu^{3+} ions are irradiated by the electron beam, the spontaneous emission of Eu^{3+} ions is mainly composed of 590 nm peak ($^5D_0 \rightarrow {}^7F_1$) and 620 nm peak ($^5D_0 \rightarrow {}^7F_2$) transitions. The radiation peaks at 590 nm and 620 nm contribute to the orange and red emission, respectively [5,17,20,21]. The CL of Eu^{3+} ions depends on the magnitude of the transition probability of luminescent ions. Although there are several types of transitions, such as an electric quadrupole and a magnetic dipole, the electric dipole transition is the most dominant. The electric dipole transition is

#145138 - $15.00 USD Received 19 Apr 2011; revised 13 Jun 2011; accepted 14 Jun 2011; published 23 Jun 2011

hypersensitive to the polarizability of the ligand and to the site asymmetry caused by the charge distribution. In addition, it can be modified by incorporating an electromagnetic wave around the atom [22]. The 590 nm peak ($^5D_0 \rightarrow {}^7F_1$) and 620 nm peak ($^5D_0 \rightarrow {}^7F_2$) of the Eu^{3+} ions are governed by the magnetic dipole and electric dipole transitions, respectively [1,5]. Modifying the probability of the electric dipole transition at 620 nm is a novel way to enhance the red emission intensity of Eu^{3+}-doped phosphor. Figure 4 shows that the enhancement at 620 nm is larger than the enhancement at 590 nm, a fact that supports our belief. The localized surface plasmon caused by the Ag nanoparticles induces the concentration and enhancement of the local electric field around the metal nanoparticles, which increases the polarizability of the ligand and the site asymmetry [23]. Figure 4(b) provides the evidence that the asymmetric ratios of samples with Ag nanoparticles increased compared to the reference. Therefore, the enhanced emission of Eu^{3+}-doped phosphor can be attributed to the resonant coupling between the localized surface plasmon and the electric dipole transition and also to the site asymmetry caused by the local field enhancement. Remarkably, the CL intensity of the samples with Ag nanoparticles increases as the thickness of the Ag nanoparticle deposition increases. It is also strange that this enhancement only occurs when a dielectric spacer is inserted between the light emitter and the Ag nanoparticles. If the light emitter is in direct contact with the Ag nanoparticles, the luminescence of the light emitter can be quenched. To prevent luminescence quenching, we deposited an MgO dielectric spacer onto the Ag nanoparticles [24,25]. In our results, the CL intensity of the Eu^{3+}-doped phosphor reaches a maximum when the MgO thickness is 20 nm and then decreases when the MgO thickness exceeds 20 nm. This behavior explains why the localized surface plasmon of the Ag nanoparticles exerts an influence within a few dozen nanometers and why the resonant effect decays exponentially [24,25]. From these results, we predict that the surface plasmon enhanced cathodoluminescence can be useful for a display device with the high luminous efficacy. In addition, the surface plasmon mediated the Eu^{3+}-doped phosphor has the advantage in sight of color purity. Since the radiation at 590 nm shows the orange emission, relatively strong emission intensity at 620 nm can contribute the pure red emission.

4. Conclusion

In conclusion, this paper is the first to report that the red emission from Eu^{3+}-doped phosphor under the pumping of an electron collision can be enhanced by coupling the localized surface plasmon resonance with the radiation energy of CL phosphor. In addition, the enhancement only occurs within a few dozen nanometers from the surface of the Ag nanoparticles, depending on the thickness of the dielectric spacer. It is greatly significant that the CL intensity can be enhanced by the localized surface plasmon caused by the metallic particles. Further work is needed to implement high luminous display devices with metallic particles, such as field emission display or a carbon nanotube backlight unit.

Acknowledgments

This research was supported by Basic Science Research Program through the National Research Foundation of Korea (NRF) funded by the Ministry of Education, Science and Technology (CAFDC-20100009890). This research was also supported by a grant (F0004072-2010-33) from Information Display R&D Center, one of the Knowledge Economy Frontier R&D Programs funded by the Ministry of Knowledge Economy of the Korean government.

#145138 - $15.00 USD Received 19 Apr 2011; revised 13 Jun 2011; accepted 14 Jun 2011; published 23 Jun 2011